ISSN 2504-9593
DOI: 10.5281/zenodo.18771014
https://ijree.com/index.php/publications/article/view/39
Int. J. Renew. Energ & Environ Vol.4 (1), pp 172-198(2026)

MODELING AND OPTIMIZATION OF PROCESS CONDITIONS INFLUENCE ON GLUCOSE, XYLOSE AND BIOETHANOL YIELD FROM LIGNOCELLULOSIC WASTE PALM FRUIT BUNCHES

Onuoha, L. N.[1], Ehiem, J. C.[2], Aviara, N. A. [2, 3*], Igbozulike, A. O.[2] Nwankwojike, B. N.[4]

[1]Department of Mechanical Engineering, Gregory University, Uturu, Nigeria
[2]Department of Agricultural and Biosystems Engineering,
Michael Okpara University of Agriculture, Umudike, Nigeria
[3]Department of Food Engineering, Michael Okpara University of Agriculture, Umudike, Nigeria
[4]Department of Mechanical Engineering, Michael Okpara University of Agriculture, Umudike, Nigeria
*Corresponding Author: aviarastar@gmail.com, nddyaviara@yahoo.com,
aviara.aviara@mouau.edu.ng

ABSTRACT

This study examined the effect of processing parameters (acid concentration, temperature and process duration) on the yield of glucose, xylose and bioethanol synthesized from lignocellulosic waste palm fruit bunches. Raw material was procured from a palm oil processing company in Port-Harcourt, Nigeria. It was mechanically communited, characterized and hydrolyzed using different concentrations of H_2SO_4, temperatures and resident times. Hydrolysates were tested for xylose and glucose yield using a spectrophotometer Hydrolysates were then fermented at room temperature for different time duration using *Saccharomyces sereviciae*. Hydrolysis and fermentation processes were modeled and optimized using the RSM. A laboratory distiller was used to purify the bioethanol obtained, and the proximate composition and fuel properties were determined. Results showed that the feedstock had a composition of 74.33 % holocellulose, (57.44 % α-cellulose and 16.89 % hemicelluloses), 15.87 % lignin and 5.57 % ash. RSM polynomial of the quadratic form adequately expressed the relationship existing between process variables and yield of glucose, xylose, and bioethanol with R^2 and SEE ranging from 0.963 to 0.993 and 0.121 to 2.501, respectively. Optimum glucose and xylose yield was 34.643g/L and 18.471g/L, at 1.196 and 1.195% acid load hydrolysis for 26.924 and 21.578 mins at 160.407 and 160.071^{o}C, respectively. Optimum bioethanol yield of 32.838 g/L was obtained at 72.933h and 86.15% fermentation efficiency. The bioethanol had 97.68 % purity, 0.03 % ash, 0.42 % moisture content, 5.05 mg/L acidity, and 6.61 pH. The fuel properties were 791.13 kg/m^3 density at 15^{o}C, 1.67 mm/s^2 viscosity at 40^{o}C, 124 Octane Number, 13.043 kPa vapour pressure, 12.8^{o}C flash point, 79 - 101^{o}C distillation temperature range, 358^{o}C auto-ignition, 29.16 MJ/kg calorific value, and 589.51^{o}C drivability index. Proximate composition of the bioethanol satisfied the ASTM D4806 specification, its fuel properties met the International Standard, therefore, it can be blended with pure petrol for use in spark ignition engines.

Keywords: Lignocellulosic biofeedstock, hydrolysis, fermentation, bioethanol, bioprocess modeling,

1.0 Introduction

Fossil fuels have been providing over 80 % of world's energy demands mainly because they are readily available and convenient to use (Holek et al., 2022). But these resources are not renewable and will eventually deplete (Suanes et al., 2024). The readily accessible reserves may well

get exhausted within the nearest future (Helma, 2013, Tan et al., 2014, Friedemann, 2021, Saud et al., 2024). Fossil fuels have high energy intensity and have heralded technological progress

but has led to air pollution, acid rain, greenhouse effect and therefore, global warming which are serious environmental threats and harmful to human health (Ahmad et al., 2022, Zhang, 2024, Wang and Azam, 2024).The continual and increasing energy demand of the world, advances in technology, uneven distribution around the globe and non-renewability of fossil fuels in addition to the rising costs of the resultant pollution, have led to desire for alternative or fuel additive. Hence, biofuels from renewable energy sources became highly needed as alternative (Ferreira et al., 2010). Due to its high-energy values, ethanol appears to be the most promising future biofuel (Ferreira et al., 2010). Ethanol energy content is about 70 % of that of petrol (Pradeep and Samir, 2011). Its reduction in greenhouse gas emission is an added value. Bioethanol is produced by pretreatment, hydrolysis and fermentation of the bio raw materials (Nuru et al., 2014, Tran et al., 2019, Vasic et al., 2021, Amraini et al., 2023). The enormous advantages of biofuels have geared research towards the production of bioethanol and other biofuels from various renewable organic raw materials. The traditional feedstocks (first generation) include cereal grains such as corn, sorghum and millet. Others are cassava, yam, cocoyam, potato, sugar cane, and sugar beets. Second generation bio feedstocks include rice straw, rice husk, wheat straw, corn cob, bagasse and wood shavings and other lignocellulosic agro wastes, while algal biomass constitutes the third-generation feedstock (Ezea, 2023).

But renewable feedstock for bioethanol production must be naturally abundant and should not compete with human food supply (Ruth 2008). Hence utilizing renewable agro wastes for second generation bioethanol production will yield double benefits in that the disposal problems of such wastes would be eliminated; the environment will be conserved and the feedstocks that are food materials (first generation) can be retained for mainly food use. It is estimated that bioethanol produced from the world's agro-wastes and forest residues could replace 32 % of global petrol consumption (Leland, 2005). Currently, there are not many wastes to ethanol production operations at commercial scale in Nigeria. One of the industries that have great potential for the utilization of their wastes in bioethanol production is the palm 0il producing industry. The Waste Palm Fruit Bunche (WPFB) is a lignocellulosic biomaterial that can function as a viable feedstock for bioethanol production, hence, its utilization in bioethanol production will enhance its disposal and maintain environmental sustainability, generate employment, enhance bioethanol fuel production, create wealth and exert positive economic impact on the society. WPFB as a lignocellulosic biomass, is composed of cellulose, hemicellulose and lignin. Of these three components, lignin has the most complex structure making it recalcitrant to both chemical and biological conversions. Pretreatment is usually applied to open up its structure and increase its digestibility and subsequently, the degree of conversion (Geng, 2013). Tran et al. (2019) noted that pretreatment processes are applied to lignocellulosic bio feedstocks prior to hydrolysis and fermentation in order to increase the amorphous region which is easier to be hydrolysed than the

crystalline cellulose, and increase the porosity of the fibre matrices to enhance the penetration of chemicals and enzymes into the structure, to liberate cellulose from the surrounding lignin and hemicellulose. Hydrolysis and fermentation of the pretreated biomass under certain processing factors, yield bioethanol. Fakruddin et al. (2012) studied the factors affecting bioethanol production by Saccharomyces Cerevisiae and noted that the key ones were temperature, pH and sugar concentration – glucose and xylose.

Several studies (Mishra and Goh, 2019, Kabue et al., 2020, Betiku and Taiwo (2015, Ebrahimiagda and Ogden, 2018, Salakkam et al., 2023) have been carried out on the production, modelling and process optimization of bioethanol from different feedstocks using different approaches. Mishra and Goh (2019) produced bioethanol from kan grass, sugar cane bagasse and wheat straw lignocellulosic feedstocks using a novel process called fractional hydrolysis and co-culture fermentation. Kabue et al. (2020) applied a second order optimal rotatable design in four dimensions to the study of the effect of four process variables namely pH, temperature, time and substrate concentration, on bioethanol yield from pineapple peels using Saccharomyces Cerevisiae, and obtained a model with high coefficient of determination indicating a good agreement between the experimental data and the predicted values. Betiku and Taiwo (2015) modelled and optimized bioethanol production from breadfruit hydrolysate using response surface methodology and artificial neural network and showed that both approaches were suitable for predicting yield from the feedstock. Ebrahimiagda and Ogden (2018) evaluated, modelled and optimized the yield efficiency of bioethanol produced from sweet sorghum juice using full factorial design and reported the process parameter levels that yielded optimum efficiency. Salakkam et al. (2023) modelled bioethanol production from sweet sorghum juice under high gravity fermentation using the Monod-based, logistic, modified Gompertz and Weibull models and noted that the Monod-based models incorporating substrate and product inhibition terms gave the higher performance in describing cell growth, Total Sugar and bioethanol concentration, and fitted data well when compared with the logistic, modified Gompertz and Weibull models.

RSM is a strong statistical analytical tool that involves the collection of mathematical and statistical techniques that are employed in constructing models and analyzing problems where the response depends on several variable factors. It is important for process optimization and enhancement of product quality with applications across scientific and industrial fields (Djimtoingar et al., 2022 and Atkinson et al., 2007). The application of RSM in process optimization and experimentation involves design of experiment, and model development. The model is normally polynomial in nature and it is used to describe the relationship exiting between the input variables (factors) and the output (Response). The effects of individual factors and their interactions on the response are estimated using iterative process and graphical representations such as contour plots and surface plots are used to visualize the

relationships between variables and the response. This procedure appears not to have been applied to the investigation of waste palm fruit bunch (WPFB) conversion to bioethanol in Nigeria. Little information also appears to be available on modelling and optimization of bioethanol yield from WPFB in the country. This study attempts to convert WPFB into wealth, and carry out an environmentally friendly mode of its disposal. Another objective of the study was to model and optimize the glucose, xylose and bioethanol yield from WPFB , a lignocellulosic palm oil mill by-product using Response Surface Methodology (RSM) with the proximate composition and fuel properties of the bioethanol produced evaluated.

2. Materials and Methods

2.1 Feedstock and Materials Procurement

The bulk quantity of waste palm fruit bunch (WPFB) used in the study was collected from the palm oil mill, SIAT Nigeria Ltd, Ubima, Rivers State, Nigeria. The bunches were shredded, cleaned and sterilized, in the course of operation of the oil mill. Waste palm fruit bunches that were less than two weeks old from the date of harvest, were used for the study. This was done to minimize the effect of post-harvest history and biochemical degradation. The chemicals used were supplied by Jucenco Enterprises, Owerri, Nigeria. These included H_2SO_4 for hydrolysis, NaOH for neutralization, distilled water, phenol and phloroglucinol for colour reagents, D-xylose and D-glucose for standard solutions, and yeast for fermentation. The reagents were used to produce Sulphuric acid solution, sodium hydroxide solution, D-xylose solution, D-glucose solution, phloroglucinol solution, chromic acid solution and phenol solution. The equipment used included electronic balance, sieve cloth, thermometer, spectrophotometer, air oven, stirring rod, pH meter, water bath, calibrated containers, pressure gauge, and laboratory distillation unit.

2.2 Experimental Design

Experimental design was carried out for glucose, xylose and total sugar yield, respectively, as responses to temperature, acid concentration and time using Box-Behnken Design, while that of bioethanol yield as a response of resident time and total sugar was carried out using Central Composite Design, all in the RSM of Design Expert 13.

2.3 Feedstock Preparation

The raw material was pretreated, hydrolysed and subjected to fermentation with the fermentate distilled to obtain pure bioethanol as described in the following sections.

2.3.1 Physical pretreatment

20 kg bags of the collected feedstock were subjected to physical pretreatment (drying and mechanical communition). The sterilized feedstock was oven dried at 60^{o}C for 3h in a 7.756 kW FRA Series of Southstar Industrial Air Oven Dryer, to 8 % moisture content on a wet basis.

The dried feedstock was ground to fine particles using a 1460 rpm / 3 HP ATLAS fiber grinding machine. The fine particles obtained were then screened with a Filterwel Test Sieve to obtain 850 microns powder (ASTM 20).

2.3.1.1 Feedstock Powder Characterization

The ground feedstock was characterized for its lignocellulosic compositions (hemicelluloses, cellulose, lignin, moisture content) following the method

of Nurul et al. (2014). The chemical compositions of pulverised WPFB were analysed according to ASTM 1104-56 and ASTM D1103-60 method for holocellulose and α-cellulose, respectively. Lignin content was determined using the gravimetric method reported by Nurul et al. (2014). This involved weighing 3 g of sample into a 100 ml Erlenmeyer flask and stirring for 2 h in 60 ml of cold 72 % (v/v) H_2SO_4 solution. The mixture was transferred into a 500 ml beaker and boiled for 4 h in a 600 ml distilled water bath under continuous stirring, and then filtered using glass microfiber filter grade GF/B (Whatman) in porcelain crucible. The residue retained was washed with hot water until it was acid free and allowed to dry at 105 °C for 2 h and weighed.

The holocellulose - a composite of cellulose and hemicellulose - was extracted from WPFB using the acidified sodium chlorite method (Nurul et al., 2014). To determine hemicelluloses, a total of 6.0 g of the holocellulose obtained was dissolved in 120 ml of 17.5 % (v/v) NaOH solution and stirred for 30 min. A total of 30 ml of NaOH solution was added into the mixture and allowed to mix to separate hemicellulose from the holocellulose and leave α-cellulose. The insoluble α-cellulose was filtered and washed separately with 8.3 % (v/v) NaOH solution followed by 10 % (v/v) acetic acid. The α-cellulose was finally washed with hot water to a neutral pH and dried overnight at 80°C (Nurul et al., 2014).

The ash content was determined using the AOAC (1980) method. Triplicate samples of 2.0 g ground WPB were weighed as W_2, into dried porcelain crucibles each having the weight W_1. The samples were charred on a heating mantle and then transferred into a muffle furnace set at 550 °C for 3 h. They were then cooled in a desiccator and finally weighed to obtain W_3. The average percentage ash was calculated using Equation 1.

$$Ash, mass\ \% = \frac{W_3 - W_1}{W_2} \quad (1)$$

where: W_1 is weight of crucible (g), W_2 is initial ground WPFB (g), W_3 is final weight of crucible and charred ground WPFB (g).

2.3.2 Dilute Acid Hydrolysis

Dilute H_2SO_4 acid was used to hydrolyze the sample following the method of Farid et al. (2010), Millati et al. (2011), Nurul et al. (2014), Akpan et al. (2005), and Kumar et al. (2009), under a controlled temperature using a 550 W, 200 V/50 Hz regulated digital oven which served as an autoclave. The oven had a temperature range of ambient +5 – 250°C with +/-1°C fluctuation. A single stage hydrolysis was carried out. The ratio of sample to acid solution was controlled at 1:10 (w/v) (Fitriani and Anwar, 2013, Mingjia et al., 2010, Nurul et al., 2014). The parameter examined was sugar yield at the resident time of 15, 37.5, 60 min, 0.8, 1 and 1.2 % acid concentration (acid % of water volume) and temperature of 160, 180 and 200°C, respectively. 200 g of the ground WPFB was mixed with 2000 ml of distilled water, and H_2SO_4 at different concentrations in cylindrical vessels made of a corrosion resistant alloy (high steel alloy).

The mixture was stirred well for homogeneity, and then hydrolyzed in a digitally controlled oven. The time of the reaction started when the reactor (oven) reached the set reaction temperature. The

acid hydrolyzed slurry was allowed to cool to room temperature in an ice bath. It was neutralized with 2M NAOH standard solution in 1dm^3 water (Cheng et al., 2007, Farid et al., 2010, Nuru et al., 2014) to 4.8pH. The filtrate was then analyzed for reducing sugar (glucose and xyloses) using a spectrophotometer (Congcong et al., 2013). The experiment was carried out in 3 replicates of each acid concentration with 10 % (w/v) solid loading for different holding times.

2.3.2.1 Glucose Determination

Glucose determination was carried out using the Phenol Sulphuric method (Duboise et al., 1956; Congcong et al., 2013). Glucose standard solutions were prepared by dissolving 1.25 g of glucose in 250 ml distilled water. Aliquots were taken from this solution to obtain 1.0, 2.0, 4.0, 8.0 and 10 ppm. 1 ml of 5 % phenol followed by 5 ml concentrated sulphuric acid added before the reading of their absorbances were taken. Solutions of known glucose concentration were taken as standard solutions; and their absorbances were used to establish the calibration curve (Figure 1) for determining the glucose content of a solution of known absorbance. To determine glucose yield, 1 ml of the hydrolyzate was mixed with 1ml of 5% phenol solution. The mixture was added 5 ml of concentrated sulphuric acid and stirred well to form the sample solution. Sample solutions were allowed for 30min to cool and the glucose yield was then measured from the absorbance at the wavelength of 488 nm. The spectrophotometer was standardized by adjusting it to zero absorbance with a reagent blank containing 1 ml of distilled water and 1 ml of 5% phenol followed by 5ml conc. sulphuric acid, before reading. Dilution with same quantity of water was carried out on the samples for readability.

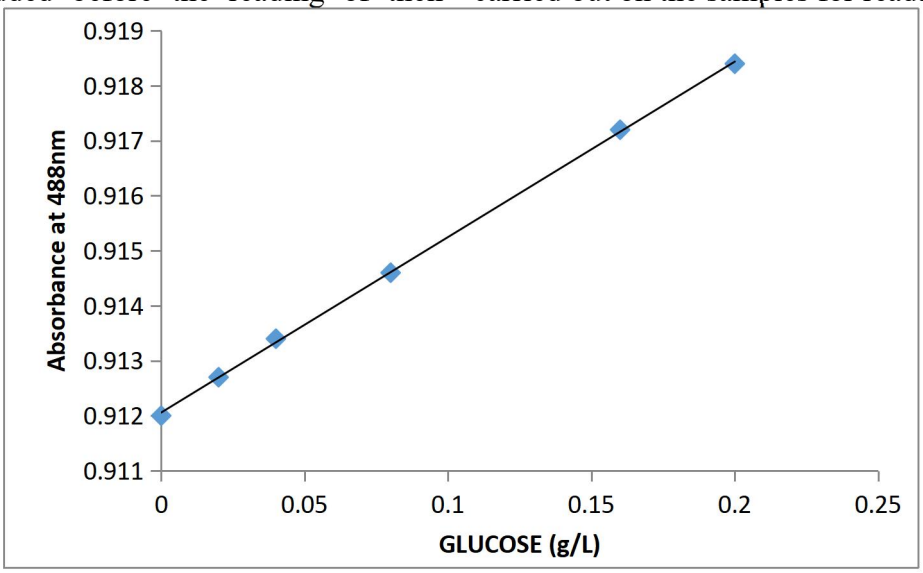

Figure 1: Absorbance of Glucose Standard Solution

2.3.2.2 Xylose Determination

Xylose determination was carried out using the colour reagent method (Miller, 1959; Congcong et al., 2013). It was based on the fact that in the solution of HCL, phloroglucinol gives colour reaction with sugars and shows maximum absorbance at 554nm wavelength for xylose (Hu et al., 2008; Browning, 1967). The colour reagent consisted of 0.5g

Phloroglucinol, 100ml of acetic acid and 10ml of concentrated HCL. Different Xylose standard solutions were prepared by dissolving 2.5 g D-xylose in saturated solution of benzoic acid to make 0.7, 1.0, 1.3, 2.6 and 3.9 mmol/L concentrations. 2 g of benzoic acid was dissolved in 200 ml hot water to obtain the saturated solution. 5 ml Phloroglucinol colour reagent was added to 5 ml of xylose standard solution and used to establish the calibration curve (Figure 2). To determine xylose content of a sample, 5 ml of Phloroglucinol colour reagent was added to 5 ml of the sample solution in a test tube, and heated for 4 minutes at 100°C in a TT - 420 Model Techmel & Techmel USA Water Bath. The mixture was cooled to room temperature. Blank solutions containing 5 ml water and phloroglucinol reagent (5 ml) were prepared by heated and cooled along with the solutions. The spectrophotometer was standardized by adjusting to zero absorbance with the reagent blank before the reading of the standard and sample solution absorbances. Xylose concentration of sample was obtained from Figure 2.

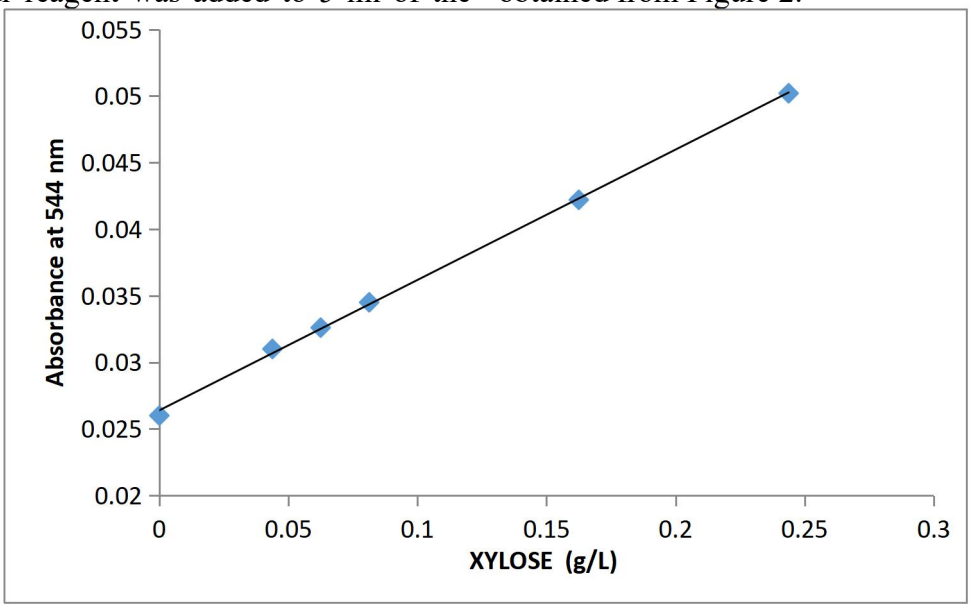

Figure 2: Absorbance of Xylose Standard Solution

2.4 Fermentation

For the fermentation process, S.sereviciae yeast was selected as the catalyst to use considering the reports of Chayanoot and Sairudee (2013) and Cheng et al. (2007) which suggested it for high ethanol yield. S.sereviciae was isolated from palm wine using Saboured Dextrose Agar (SBA). This was carried out by inoculating 0.1 ml aliquot of 10^{-2} dilution of freshly tapped palm wine and incubating the already inoculated plates at 27°C for 24 h. At the end of the inoculation period, the isolated yeast was characterized using morphological and Lactophenol cotton blue staining technique. Thereafter, a loopful of the identified yeast was subcultured into 60ml of nutrient broth contained in a test tube and incubated at 27°C for 24 h.

Hydrolysates obtained from WPFB with highest glucose values were fermented at room temperature and pH condition of about 4.8 which gave optimum salinity for yeast growth (Liu and Chen 2008). 100 ml of the prepared yeast innoculum was aseptically inoculated unto the hydrolysates in 12 L containers sealed

with Vaseline petroleum jelly and nylon material to prevent the diffusion of air into the setup, but allow the exit of CO_2. Aliquot was collected at 24 h interval of sugars consumption for 72 h, filtered and analyzed for bioethanol yield. Fermentation process was terminated using 0.5ml HCL when bioethanol yield began to decline. Bioethanol yield with time was recorded.

2.5 Bioethanol Determination

Total bioethanol concentration in the filtrate medium was estimated by Chromic acid method and measuring absorbance at 584 nm wavelength using a spectrophotometer (Caputi et al., 1968, Congcong et al., 2013). Chromic acid reagent was prepared by dissolving 34 g of potassium dichromate in 500 ml of distilled water. 325 ml of concentrated H_2SO_4 was added and the volume was made up to 1000 ml. Bioethanol was estimated calorimetrically as described by Caputi et al. (1968). 1ml of sample in a test tube was made up to 5 ml with distilled water, 5 ml of the chromic acid was added, after which the test tube was incubated in a water bath at 60°C for 20 min. The absorbance was determined in a spectrophotometer at 584 nm and converted to bioethanol concentration from the calibration curve produce using standard solution of absolute ethanol (Figure 3).

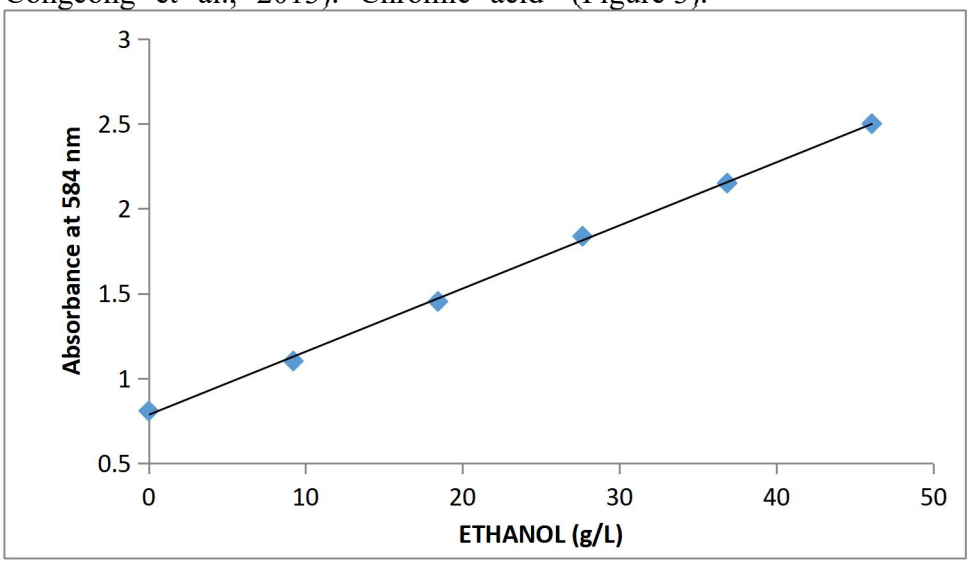

Figure 3: Absorbance of Standard Ethanol Solution

Fermentation yield which is the actual bioethanol yield after fermentation was expressed using Equation (2) due to Nurul et al. (2014) as:

$$Bioethanol\ yield\ (g/L) = \frac{bioethanol(g/L)}{Glucose\ (g/L)} \quad (2)$$

Theoretically, 1g glucose and xylose yields 0.511g of ethanol (Mingjia et. al., 2010, Yanni et. al., 2013, Christos et. al., 1996). Also, 100 kg sugar (glucose, fructose) will yield approximately 51kg or 64.5 liters alcohol (Stephen et. al., 2013).

Fermentation efficiency was calculated using Equation (3) due to Mohd et al. (2011) and Nurul et al. (2014):

$$\text{fermentation efficiency}(\%) = \frac{\text{Bioethanol yield } x\ 100}{0.5111 Glucose\ yield} \quad (3)$$

2.6 Bioethanol Purification

It was considered that distilling the whole slurry will definitely affect clear separation of the fermented portion of the

feed and invariably affect the final yield. Thus, the feed was separated from the slurry by filtering. The initial temperature was room temperature (28 – 30 ^{o}C) and the volume of feed was noted. Laboratory distillation unit was used to isolate, confirm and purify the bioethanol present. The distillation flask was charged with the feed and heated to bioethanol boiling point of 78 ^{o}C to cause distillation. Condensed bioethanol flowed down the condenser into a measuring cylinder and was collected.

2.7 Bioethanol Characterization

Elemental analysis of bioethanol produced from WPFB was carried out as reported by Igbokwe et al. (2019) following the ASTM standard test procedure and compared to ASTM D4806 specification for denatured fuel bioethanol blendable with petrol for use as automotive SI engine fuel. Elemental properties evaluated included ash content, water content, acidity, pH and purity. The purity of the fuel was determined according to ASTM D 5501 using gas chromatography. pH was determined at room temperature using a pH meter according to ASTM D 6423. Ash content was determined according to ASTM D 482. Acidity was determined according to ASTM D 974 using Potassium hydroxide (KOH) as the titrant. Water content of the bioethanol was determined based on ASTM D 95.

Fuel property analysis was carried out on the produced bioethanol. The properties include kinematic viscosity, flash point, density, octane number, calorific value and Vapor pressure. The density @ 15^{o}C was determined according to ASTM D 4052. Viscosity @ 40^{o}C was determined according to ASTM D 445. Octane number (ON) was determined according to ASTM D 2699. Vapour pressure was determined according to ASTM D 4953. Flash point was determined according to ASTM D 93. Distillation temperature range was determined according to ASTM D 86. The auto ignition point was measured according to the procedure described in ASTM E 659. Calorific value was determined according to ASTM D 240. Drivability index was determined according to ASTM D 4814.

2.8 Data and Analysis

All the investigations were carried out in triplicate and the average values are reported. Data obtained on glucose, xylose and total sugar yields were modeled with the input factors taken as temperature, acid concentration and time, while bioethanol yield was modeled with total sugar and time taken as the input factors. All modeling operations were carried out using Response Surface Methodology in Design Expert. The polynomial model of the second order was applied to the data to express the responses as a function of the input variables. Model goodness of fit was determined using coefficient of determination (R^2) and standard error of estimate (SEE). ANOVA of the responses with the input variables, model diagnostics and 3D-plots were used to evaluate the models. Numerical optimization in the RSM was applied to the optimization of glucose, xylose, total sugar and bioethanol yields of WPFB under the specified process conditions. The software optimized the production processes by expressing the maximization of the responses at the optimum conditions with the ranges of process parameters.

3. Results and Discussion

The results obtained in the study are presented and discussed as follows.

3.1 Feedstock Characterization

The feedstock composition is presented in Table 1. It consists of 74.33 % holocellulose, (57.44 % α-cellulose and 16.89 % hemicelluloses), 15.87 % lignin and 5.57 % ash. This indicates that 1 kg of ground sample will have 574.4 g cellulose and 168.9 g hemicelluloses, while a ton will contain 574.4 kg cellulose and 168.9 kg hemicelluloses. Analysis of the feedstock shows that theoretical fermentable sugars accounted for more than 62.1 % on a dry matter basis, indicating that WPFB has a great potential as a bio-fuel feedstock.

Table 1: Feedstock (WPFB) Properties after Physical Pretreatment

Chemical composition	Percentage (wt %, dry basis)
Holocellulose	74.33
α-cellulose	57.44
Hemicellulose	16.89
Lignin	15.87
Ash	5.57

The holocellulose content agreed well with the report of Nor et al. (2012), Umikalsom et al. (1997), and Nuru et al. (2014). However, 5.57 % ash content and 15.87 % lignin content are higher than the findings of the above investigators, though Richana et al. (2015) reported 50.03 % ash. Also, the lignin content is high and comparable with other biomasses for example, barley straw had lignin content of 6.3 - 9.8 % (Garda et al., 2006), rice straw 17 - 19 % (Prassad et al., 2007), oilseed rape 14.2 % and winter rye 16.1 % (Petersson et al., 2007).

3.2 Glucose, Xylose, Total Sugar Yield and Optimization

Sample solutions of known absorbance were compared with standard plots (Figures 1 and 2) and applied to obtain the glucose, xylose and total sugar contents, respectively. Figure 4 shows that maximum glucose yield was 34.613 g/L obtained with 1.2 % (v/v) H_2SO_4 at 160^oC, and 30 min. At some given temperatures and acid concentrations, glucose yield increased with time to peak values after which it decreased with further increase in residence time. At other temperatures and acid concentrations it decreased steadily with time. Increase in glucose yield may be due to rapid conversion of the amorphous region and acid breakdown of the crystalline region of the cellulosic material when the amount of inhibitors are not yet significant, while the decrease in yield may be due to increase in the amount of inhibitors present in the system with time.

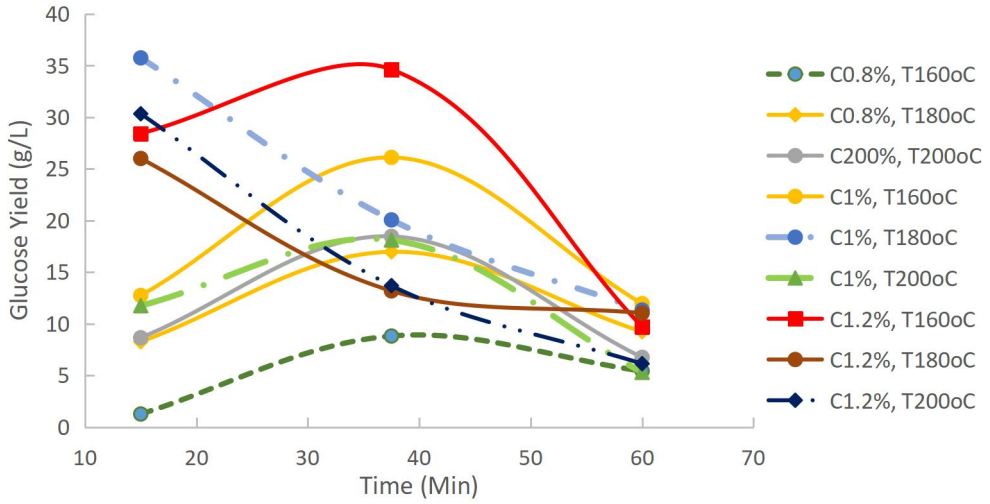

Figure 4: Glucose yield with time from hydrolysis of WPFB at different acid concentrations and temperatures

The relationship existing between glucose yield from WPFB and the hydrolysis process parameters of temperature, acid concentration and time can be represented by the model Equation (4).

$$GY = -569.01629 + 4.03037T + 362.25573C + 2.39525t - 1.95541TC - 0.002948Tt - 0.885278Ct - 0.005779T^2 + 24.36812C^2 - 0.014606t^2, R^2 = 0.9926,\ C.V = 3.01\%, SEE = 0.5453 \quad (4)$$

where: GY is glucose yield (g/L), T is temperature (°C), C is acid concentration (%) and t is time (Min).

The high R^2 and low SEE as well as the nature of the plot of the predicted versus observed glucose yield (Figure 5) for Equation (4) show that the model can be used to adequately predict the yield of glucose from WPFB at specified process conditions. The data points of the plot of predicted against the observed values are very close to the fitted straight line confirming the high accuracy of the model in predicting the glucose yield of WPFB. This is further confirmed by the result of the ANOVA of glucose yield with temperature, acid concentration and time presented in Table 2, which shows that the model is significant and that all the parameters, their interactions and the square of their values made statistically significant contributions to the predictive capability of the model. The 3D surface plot of glucose yield against temperature and acid concentration is shown in Figure 6.

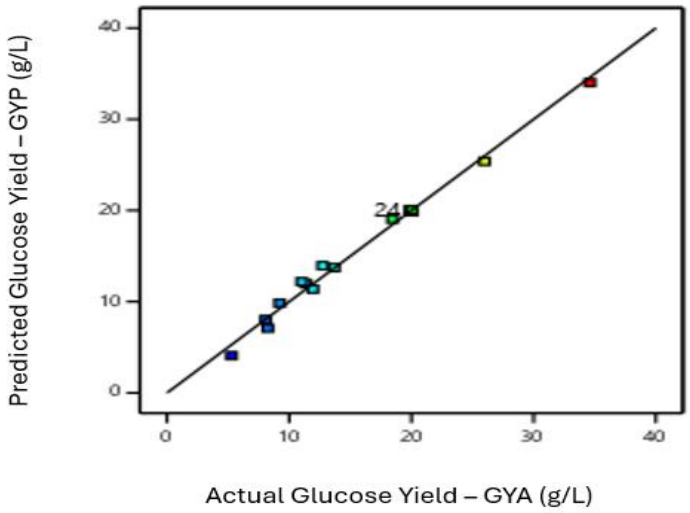

Figure 5: Plots of the predicted glucose yield against the observed value

Table 2: ANOVA of Glucose yield of WPFB with temperature, acid concentration and time

Source	Sum of Squares	DF	Mean Square	F Value	Prob > F	
Model	1039.52	9	115.50	388.55	< 0.0001	Significant
T	43.07	1	43.07	144.88	< 0.0001	
C	213.35	1	213.35	717.71	< 0.0001	
t	54.57	1	54.57	183.56	< 0.0001	
TC	244.71	1	244.71	823.20	< 0.0001	
Tt	7.04	1	7.04	23.67	< 0.0001	
Ct	63.48	1	63.48	213.55	< 0.0001	
T^2	27.00	1	27.00	90.82	< 0.0001	
C^2	4.80	1	4.80	16.15	0.0004	
t^2	276.27	1	276.27	929.36	< 0.0001	
Residual	7.73	26	0.2973			
Lack of Fit	7.73	3	2.58			
Pure Error	0.0000	23	0.0000			
Cor Total	1047.25	35				

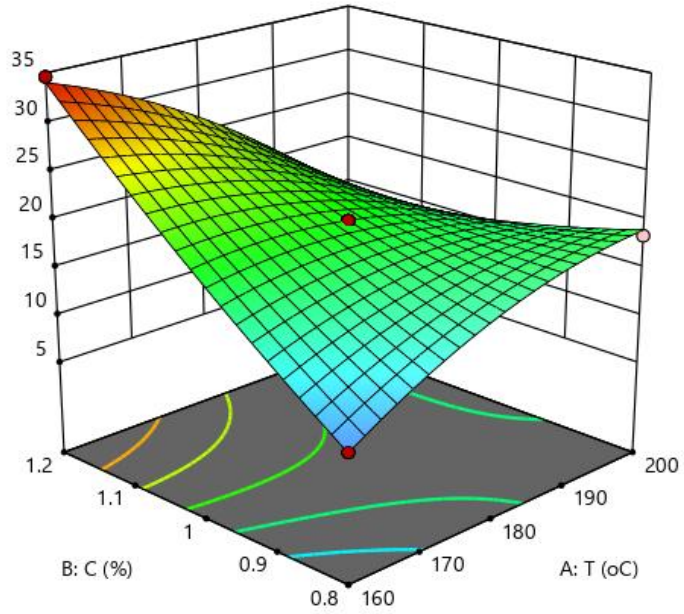

Figure 6: 3-D plot of glucose yield against temperature and acid concentration

The outcome of process optimization for glucose yield presented in Figure 7 shows that the optimum yield was 34.615g/L obtained at the temperature, acid concentration and time value of 160.407°C, 1.1986% and 26.924 minutes, respectively.

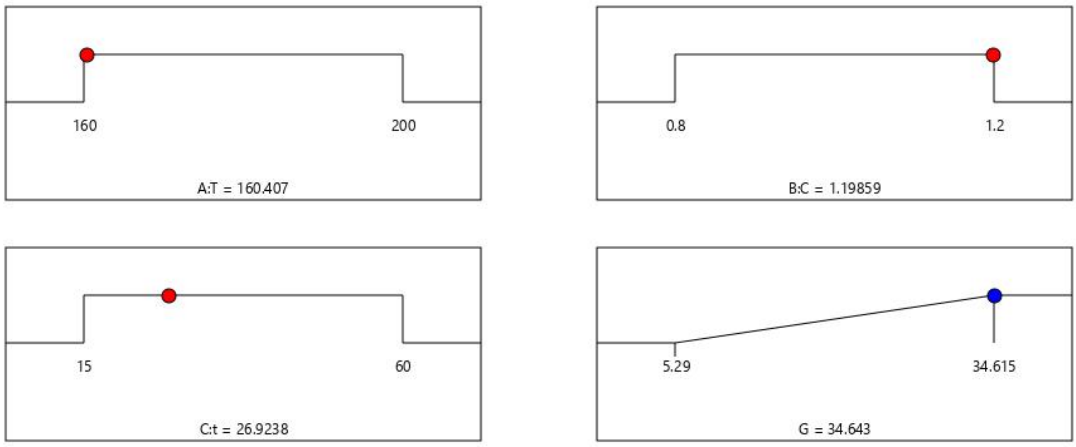

Figure 7: Process optimization of glucose yield from WPFB

Figure 8 shows that the maximum xylose yield was 18.374 g/L at 160ºC, 1.2% acid concentration and 37.5 min duration. In the above process condition, xylose yield from WPFB initially increased with time up to a point and decreased with further increase in time. Similar trend as the above was exhibited at 180ºC, 0.8%, 200ºC, 0.8% and 200ºC, 1.0% temperature and acid concentration, respectively but with lower yields. At the conditions of 200ºC, 1.2%, 180ºC, 1.0%, 160ºC, 1.0% and 160ºC, 0.8%, the yield decreased continually, and at the conditions of 180ºC, 1.2%, the yield increased continually but did not reach the maximum value. Increase in xylose yield may be due to increase in the

conversion of the amorphous region and the breakdown of the crystalline region of the cellulosic material by acid. Low xylose yield may be due to xylose degradation as reaction temperature exceeded 140°C. It can then be deduced that lower temperature (100 – 140°C) is better applied in the hydrolysis of hemicelluloses while higher temperature (180 - 250°C) can be applied in cellulose hydrolysis. The results suggest that for WPFB, low and high acid concentration favours xylose yield but at mild and low temperatures, respectively.

The relationship existing between xylose yield and the hydrolysis process parameters of temperature, acid concentration and time can be expressed with the model Equation (5).

$$XY = 14.27202 - 0.053037T - 0.271812C + 0.081314t - 0.441844TC + 0.000125Tt - 0.102467Ct + 0.001353T^2 + 44.10125C^2 - 0.000199t^2, R^2 = 0.9916,\ C.V = 0.89\%, SEE = 0.1212 \quad (5)$$

where: XY is xylose yield (g/L), T is temperature (°C), C is acid concentration (%) and t is time (Min).

Equation (5) has high R^2 and low SEE with the nature of the plots of predicted versus observed xylose yield (Figure 9) that show that the model can be used to adequately predict the yield of xylose from WPFB at specified process conditions. The data points of the plot of predicted against the observed values are very close to the fitted straight line confirming the high accuracy of the model in predicting the xylose yield of WPFB. This is further confirmed by the result of the ANOVA of xylose yield with temperature, acid concentration and time presented in Table 3, which shows that the model is significant and that acid concentration, time, interactions of temperature and acid concentration, acid concentration and time, the square of temperature and acid concentration all made statistically significant contributions to the predictive potential of the model, while temperature, the interaction of temperature and time, and the square of time had no significant effect on the model's predictive capacity. The 3-D surface plot of xylose yield against temperature and acid concentration is shown in Figure 10.

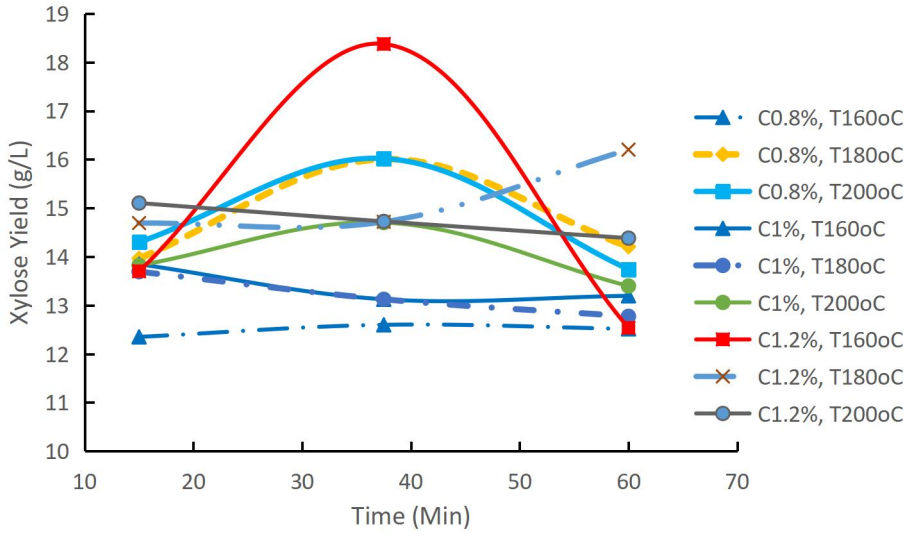

Figure 8: Xylose yield with time from hydrolysis of WPB at different acid concentrations and temperatures

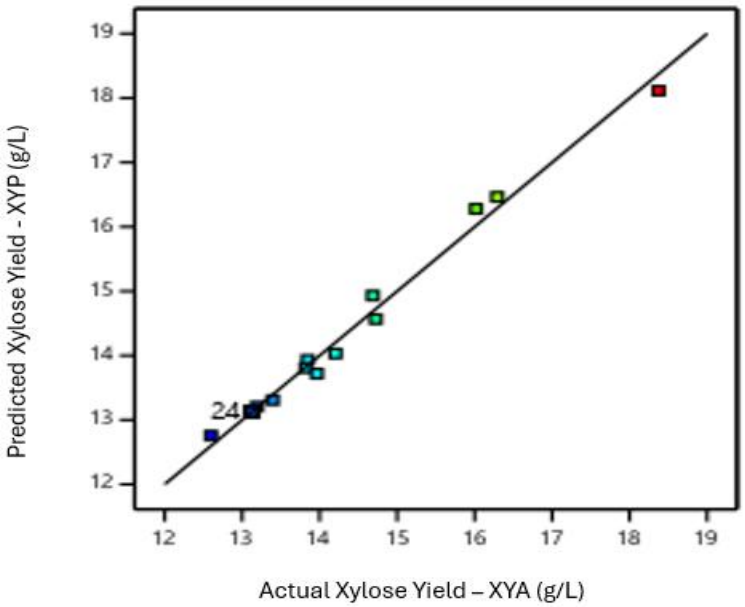

Figure 9: Plots of the predicted xylose yield against the observed value

Table 3: ANOVA of xylose yield of WPFB with temperature, acid concentration and time

Source	Sum of Squares	DF	Mean Square	F Value	Prob > F	
Model	45.21	9	5.02	342.17	< 0.0001	Significant
T	0.0003	1	0.0003	0.0225	0.8819	
C	6.64	1	6.64	452.54	< 0.0001	
t	0.7440	1	0.7440	50.68	< 0.0001	
TC	12.49	1	12.49	851.14	< 0.0001	
Tt	0.0127	1	0.0127	0.8629	0.3615	
Ct	0.8505	1	0.8505	57.93	< 0.0001	
T^2	1.48	1	1.48	100.86	< 0.0001	
C^2	15.72	1	15.72	1071.08	< 0.0001	
t^2	0.0512	1	0.0512	3.49	0.0732	
Residual	0.3817	26	0.0147			
Lack of Fit	0.3817	3	0.1272			
Pure Error	0.0000	23	0.0000			
Cor Total	45.59	35				

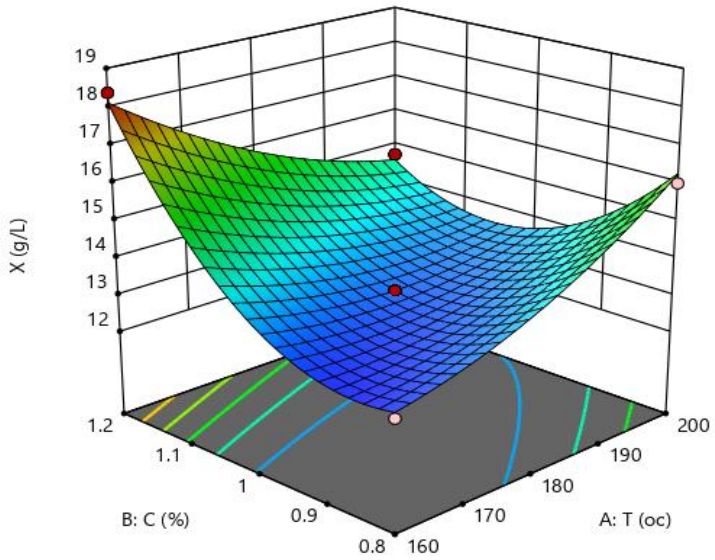

Figure 10: 3-D plot of xylose yield against temperature and acid concentration

The outcome of process optimization for xylose yield presented in Figure 11 shows that the optimum yield was 18.4712g/L obtained at the temperature, acid concentration and time value of 160.071°C, 1.19494% and 21.5775 minutes, respectively.

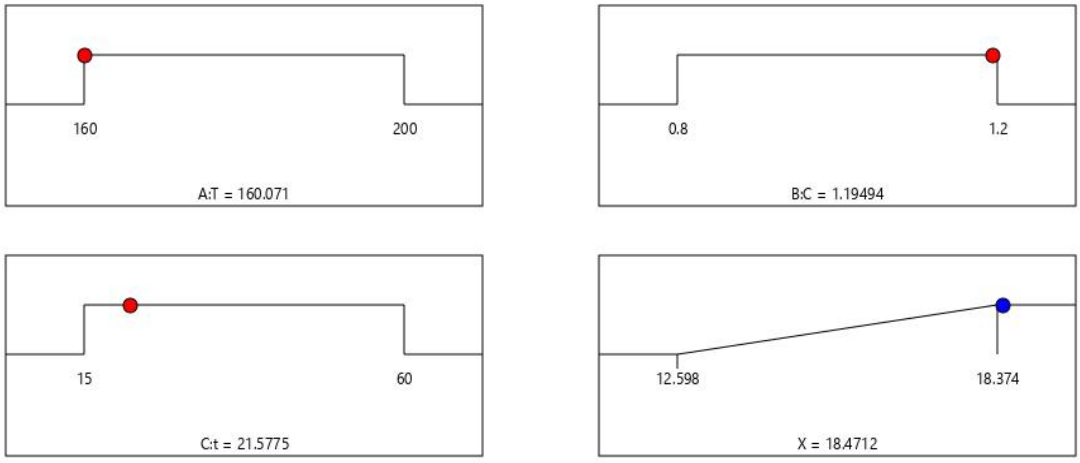

Figure 11: Process optimization of xylose yield from WPFB

Figure 12 shows that the maximum total sugar yield of 52.987g/L was obtained at 160°C, 1.2 % acid concentration and time of 37.5 min The total sugar yields are more of glucose than xylose. This explains the similarity in shape between Figures 4 and 12, and may be an indication of higher glucose content than xylose in the WPB. Glucose and xylose yields do not appear to have been favored by high temperature.

The relationship existing between total sugar yield and the hydrolysis process parameters of temperature, acid concentration and time can be represented with model Equation (6).

$$TSY = 33.17 - 2.30T + 6.05C - 2.92t - 9.64TC - 1.27Tt - 4.44Ct + 1.74T^2 + 2.77C^2 - 7.52t^2, R^2 = 0.9923, C.V =$$

$1.90\%, SEE = 0.6038$
(6)

where: TSY is Total Sugar yield (g/L), T is temperature (°C), C is acid concentration (%) and t is time (Min).

The high R^2 and low SEE as well as the nature of the plot of the predicted versus observed Total Sugar yield (Figure 13), for Equation (6) show that the model can be used to adequately predict the Total Sugar yield of WPFB at specified process conditions. The data points of the plot of predicted against the observed values are very close to the fitted straight line confirming the high accuracy of the model in predicting the Total Sugar yield. This is further confirmed by the result of the ANOVA of Total Sugar yield with temperature, acid concentration and time presented in Table 4, which shows that the model is significant and that all the parameters, their interactions and the square of their values made statistically significant contributions to the predictive capability of the model. The 3D surface plot of Total Sugar yield against temperature and acid concentration is shown in Figure 14.

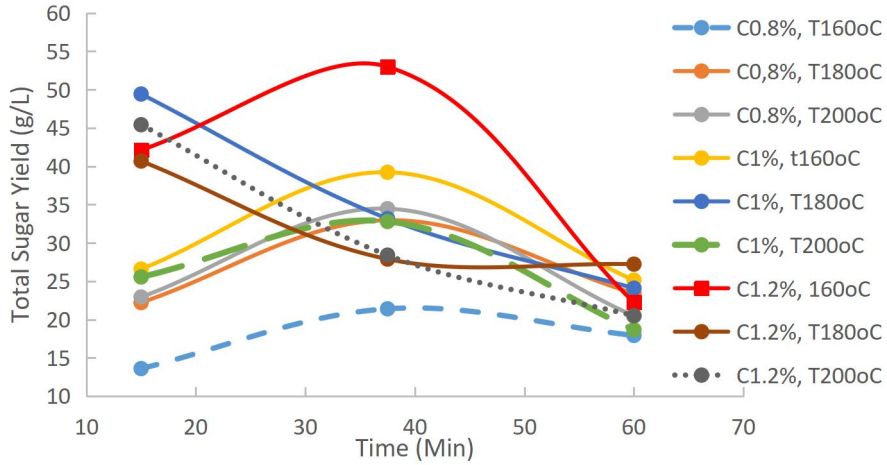

Figure 12: Total sugar yield with time from WPB hydrolysis at different acid concentrations and temperatures

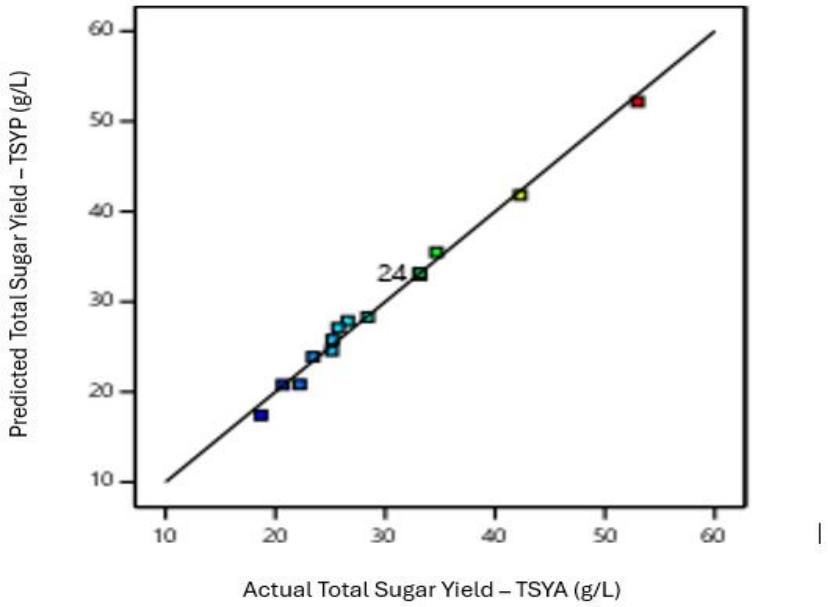

Figure 13: Plots of the predicted Total Sugar yield against the observed value

Table 4: ANOVA of Total Sugar yield of WPFB with temperature, acid concentration and time

Source	Sum of Squares	DF	Mean Square	F Value	Prob > F	
Model	1223.06	9	135.90	372.63	< 0.0001	Significant
T	42.38	1	42.38	116.22	< 0.0001	
C	292.86	1	292.86	803.05	< 0.0001	
t	68.05	1	68.05	186.61	< 0.0001	
TC	371.64	1	371.64	1019.06	< 0.0001	
Tt	6.45	1	6.45	17.69	0.0003	
Ct	79.03	1	79.03	216.70	< 0.0001	
T²	15.36	1	15.36	42.12	< 0.0001	
C²	38.64	1	38.64	105.96	< 0.0001	
t²	285.60	1	285.60	783.14	< 0.0001	
Residual	9.48	26	0.3647			
Lack of Fit	9.48	3	3.16			
Pure Error	0.0000	23	0.0000			
Cor Total	1232.54	35				

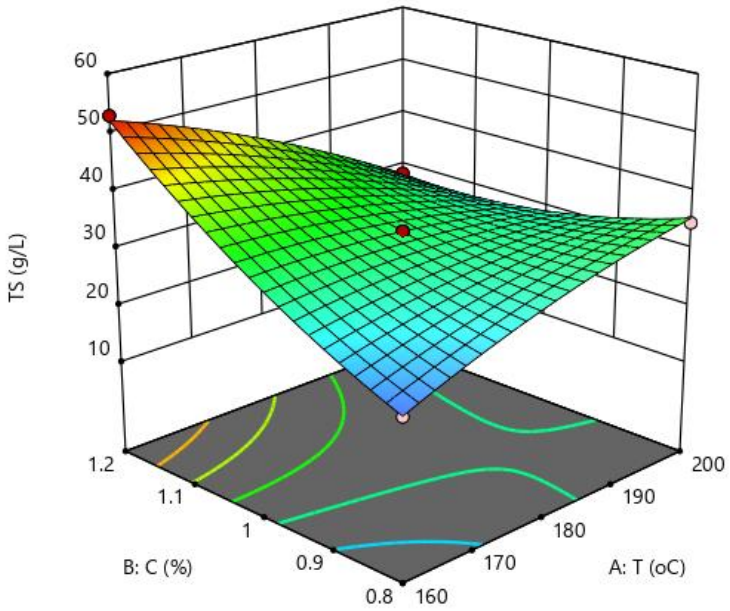

Figure 14: 3-D plot of glucose yield against temperature and acid concentration

The outcome of process optimization for Total Sugar yield presented in Figure 15 shows that the optimum yield was 53.0353g/L obtained at the temperature, acid concentration and time value of 160.47°C, 1.19889% and 30.4858 minutes, respectively.

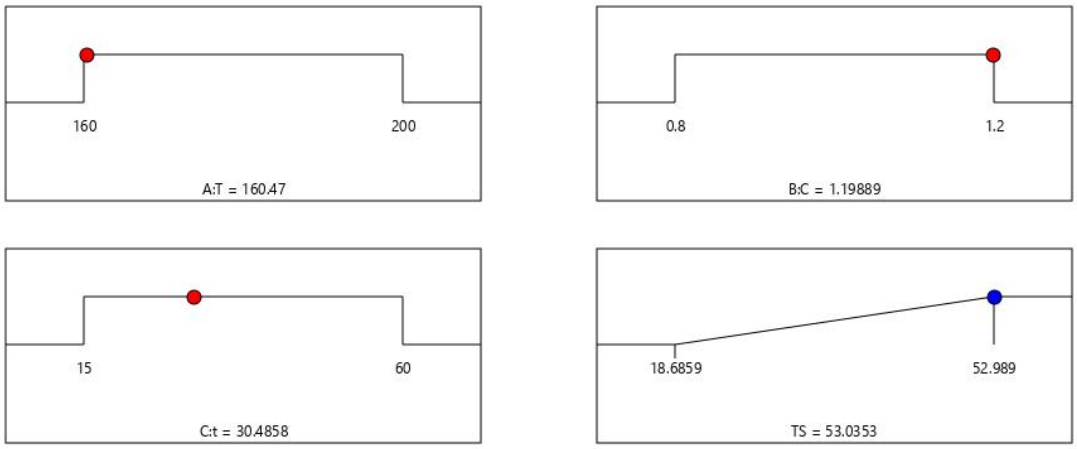

Figure 15: Process optimization of Total Sugar yield from WPFB

3.3 Bioethanol Yield and Optimization

The variation of bioethanol yield with time from fermentation of WPFB is presented in Figure 16. It was observed that samples with higher sugar concentration resulted in higher yield of bioethanol; and this confirms that carbon sourced from the sugar is the nutrient for yeast fermentation process. The available total sugar was considerably fermented.

The relationship existing between bioethanol yield and fermentation process parameters of time and total sugar yield can be expressed using model Equation (7).

$$BY = 26.10291 - 0.282028t - 1.45053TS + 0.014865tTS + 0.000044t^2 + 0.016988TS^2, R^2 = 0.9627,\ C.V = 20.72\%, SEE = 2.501 \quad (7)$$

where: BY is Bioethanol yield (g/L), t is time (hr) and TS is Total Sugar yield (g/L).

Equation (7) has high R^2 and low SEE with the nature of the plots of predicted versus observed bioethanol yield (Figure 17) all show that the model can be used to adequately predict the yield from WPFB at specified process conditions. The data points of the plot of predicted against the observed values are very close to the fitted straight line confirming the high accuracy of Equation (7) in predicting the bioethanol yield of WPFB. This is further confirmed by the result of the ANOVA of bioethanol yield with time and Total Sugar yield presented in Table 5, which shows that the model is significant and that time, Total Sugar yield, interactions of time and Total sugar yield, and square of Total Sugar yield all made statistically significant contributions to the predictive potential of the model, while the square of time had no significant effect on the model's predictive capacity. The 3-D surface plot of bioethanol yield against time and Total Sugar yield is shown in Figure 18.

Fermentation of the hydrolyzates with S.sereviciae for 72 h at room temperature gave optimum bioethanol yield of 32.8376 g/L (Figure 19), and that is 86.15 % fermentation efficiency.

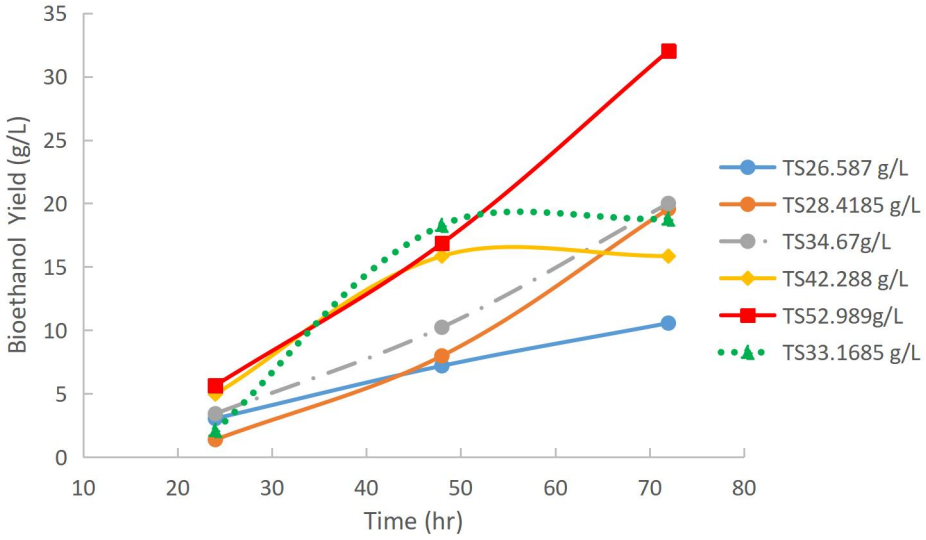

Figure 16: Bioethanol yield from WPFB fermentation with time for different Total Sugar yields

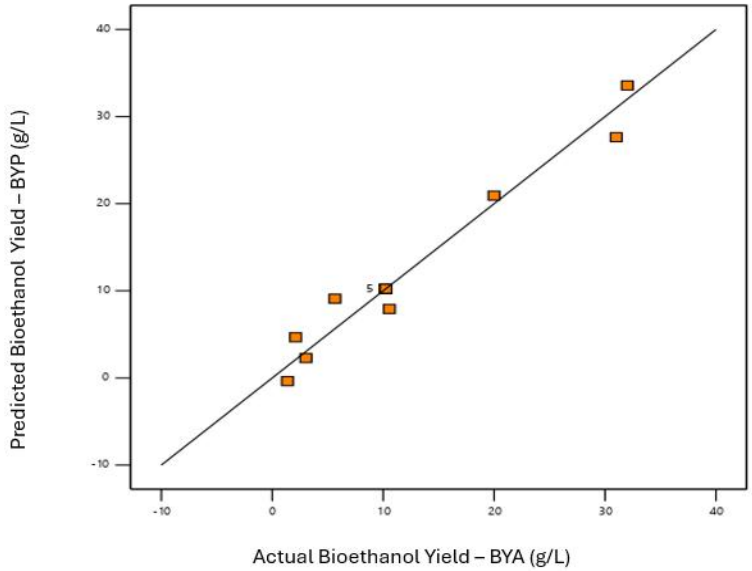

Figure 17: Plots of the predicted Biioethanol yield against the observed value

Table 5: ANOVA of Bioethanol yield of WPFB with time and Total Sugar yield

Source	Sum of Squares	DF	Mean Square	F Value	Prob > F	
Model	1130.78	5	226.16	36.15	< 0.0001	Significant
t	453.20	1	453.20	72.44	< 0.0001	
TS	526.97	1	526.97	84.23	< 0.0001	
tTS	88.72	1	88.72	14.18	0.0070	
t²	0.0044	1	0.0044	0.0007	0.9796	
TS²	60.97	1	60.97	9.75	0.0168	
Residual	43.79	7	6.26			
Lack of Fit	43.79	3	14.60			
Pure Error	0.0000	4	0.0000			
Cor Total	1174.57	12				

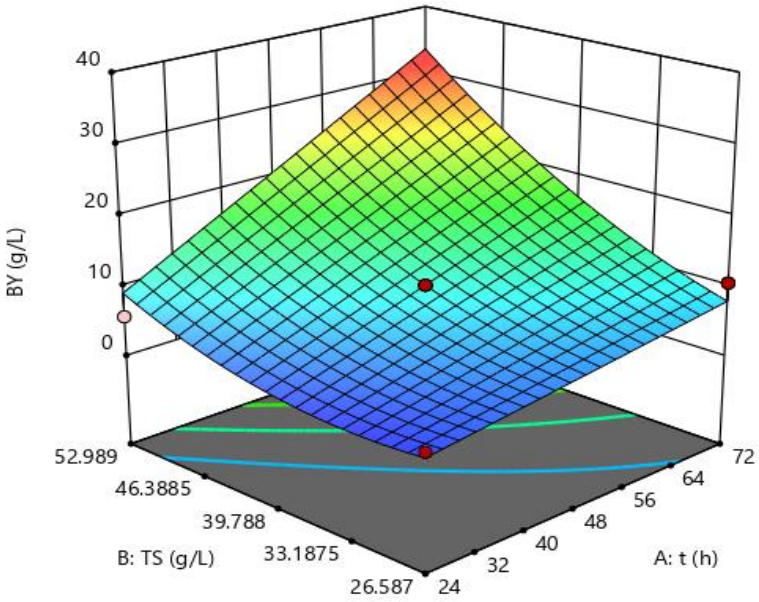

Figure 18: 3-D plot of glucose yield against temperature and acid concentration

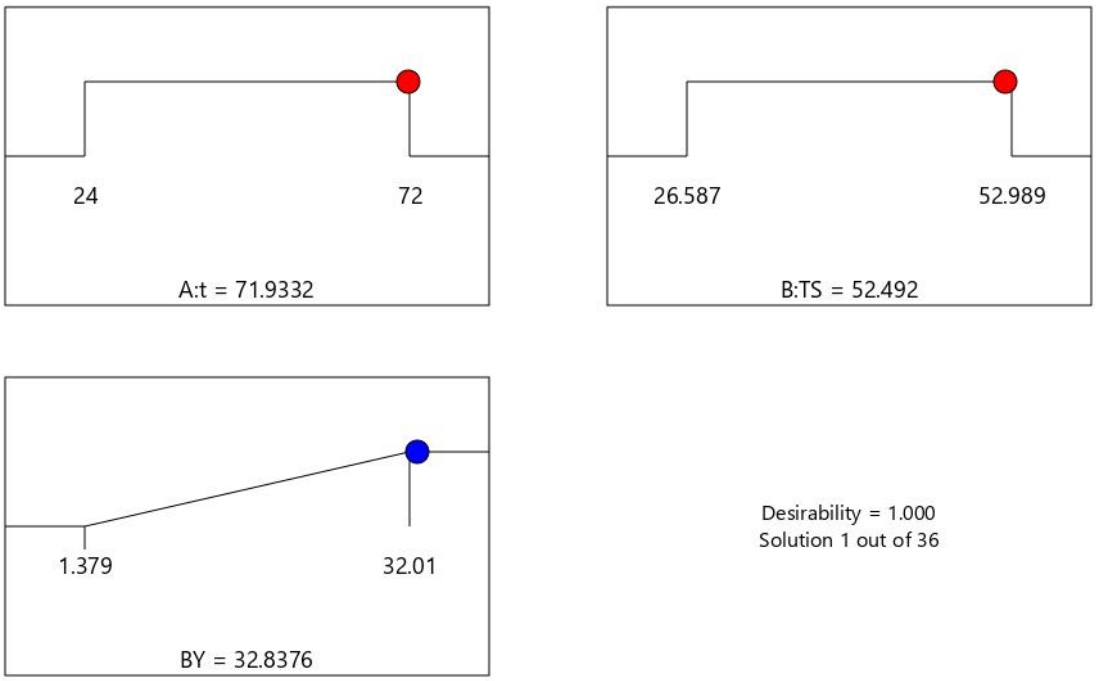

Figure 19: Process optimization of Bioethanol yield from WPFB

3.4 Elemental Composition of Synthesized Bioethanol

The result of ssynthesized bioethanol elemental analysis is presented in Table 6 and compared with the ASTM D4806 specification for fuel ethanol. From the Table, it can be seen that bioethanol from WPFB satisfied the ASTM D4806 requirement, confirming that the produced bioethanol can be blended with pure petrol for use in spark ignition engines.

Table 6: Elemental Composition of Bioethanol (E100) from WPB

Parameters	E100	ASTM Range	ASTM Method
Purity (%)	97.68		D 5501
Ash content (%)	0.03	0.05 (max)	D 482
H_2O content (% vol)	0.42	1.0 (% vol) or 1.26 mass % (max)	D 95
Acidity (mg/L)	5.05	0.007 % mass or 56 mg/L (max)	D 974
pH	6.61	6.5 – 9.0	D 6423

3.5 Fuel Properties of Synthesized Bioethanol

The result of synthesized bioethanol fuel properties analysis is presented in Table 7 and compared with the ASTM specification for fuel ethanol. The produced bioethanol has high viscosity which rules out poor atomization. It also has high Octane Number which means more efficient ignition and consequently, higher engine performance. This suggests that it can function as an effective compound for improving petrol fuel quality, therefore, it can be blended with petrol for use in spark ignition engines.

Table 7: Fuel Properties of the Bioethanol Fuel produced from WPB

Parameter	Petrol (E0)	WPB bioethanol (E100)	ASTM Method
Density @ 15^{o}C (kg/m^{3})	744.73	791.13	D 4052
Viscosity (mm/s^{2}) @ 40^{o}C	0.6097	1.6692	D 445
Octane Number	89.2	124	D2699
Vapour Pressure (kPa)	48.1	13.043	D4953
Flash point(^{o}C)	-69	12.8	D93
Distillation Temp. range (^{o}C)	44- 205	79- 101	D86
Auto-ignition (^{o}C)	245	358	D
Calorific value (MJ/kg)	43.62	29.16	D240
Drivability Index (^{o}C)	723.84	589.51	D4814

4. Conclusion

This study addressed the production of bioethanol from Nigerian Waste Palm Fruit Bunch (WPFB). The influence of process conditions on the yield of glucose, xylose, total sugar and bioethanol was modeled and optimized, and the following conclusions were drawn. The WPFB feedstock has higher percentage of cellulosic component than lignin and ash. Physical pretreatment via size reduction of the bunch opened up the structure of the recalcitrant lignin component of the biomass and enabled acid hydrolysis of the feedstock to be enhanced. At the low temperature of 160oC and high acid concentration of 1.2%, glucose, xylose and total sugar yield was maximum and they each increased with time to a peak value after which they decreased with further increase in residence time. Highest total sugar yielding hydrolysate gave the maximum bioethanol yield which increased with time during the *S.sereviciae* catalyzed fermentation process. The RSM model of the quadratic form applied, adequately expressed the glucose, xylose and bioethanol yields from WPFB as a function of temperature, acid load and resident time, and total sugar and time, respectively. Optimum glucose, xylose and total sugar yields were obtained at similar process conditions and optimum bioethanol yield was higher than the maximum and it was obtained with process parameters lower than the maximum values. Bioethanol from WPFB was of high purity (97.68%). It had ash, moisture, acidity and pH which is respectively, within the standard range. The viscosity, Octane Number, other fuel properties of the bioethanol suggest that it can function as an effective compound for improving petrol fuel quality, and it is recommended that the WPFB bioethanol-petrol blends can be used in spark ignition engines.

Acknowledgement

The authors are grateful to the Chemical Laboratory staff members of Nigeria National Petroleum Corporation (NNPC), Port Harcourt, Rivers State, Nigeria; Engr. James Oko of Jach Petro Analytical Laboratory Limited, Port Harcourt, Rivers State, Nigeria, and Emurigho Tega Anthony of the Federal Polytechnic Nekede, Imo State, Nigeria, for the assistance they rendered during the study.

References

Abdullah, N., Sulaiman, F. and Gerhauser, H. (2011). Characterization of oil palm empty fruit bunches for fuel application. *Journal of Physical Science*, 22: 1–24.

Ahmad, M., Khan, I., Qaiser, M., Khan, S. and Jabeen, G. (2022). Households ′ perception-based factors influencing biogas adoption: Innovation diffusion framework. *Energy*, 263: 126155. https://doi.org/10.1016/j.energy. 022.126155.

Akpan, U., Kovo, A., Abdullahi, M. and Ijah, J. (2005). The Production of Ethanol from Maize Cobs and Groundnut Shells. *Australian Journal of Technology (AU.J.T.)*, 1(2): 106 - 110.

Amraini, S. Z., Sari, S., Andrio, D., Fatra, W. and Susanto, R. (2023). Optimizing raw material pretreatment for bioethanol production from empty fruit bunches: A comparative study. *Grimsa Journal of Science, Engineering and Technology*, 1(1): 17-23., doi.10.61975/gjset.v1i1.

Atkinson, A. C., Donev, A. N. and Tobias, R. D. (2007). Optimum Experimental Designs, with SAS. Oxford University Press. New York, pp. 511.

Betiku, E. and Taiwo, A. E. (2015). Modeling and optimization of bioethanol production from breadfruit starch hydrolysate vis-à-vis response surface methodology and Artificial Neural Network. *Renewable Energy*, 74: 87-94.

Browning, B. (1967). Determination of Sugars: Methods of Wood Chemistry, Wiley, New York, 1: 598 - 599.

Caputi, A., Ueda, M. and Brown, T. (1968).Spectrophotometric Determination of Ethanol from Wine. *American Journal of Enology. Viticulture*, 19: 160 - 165.

Chayanoot, S. and Sairudee, D. (2013). Fermentation of Oil Palm Empty Fruit Bunch Hydrolysate to Ethanol by Baker's Yeast and Long-Pang. *PSU-UNS International Conference on Engineering and Technology*, No. T2-2.1: 1- 3.

Cheng, C., Hajar, H. and Ku, S. (2007). Production of bioethanol from oil palm empty fruit bunch. International Conference Symposium (ICoSM). University of Malaysia Pahang. http://umpir.ump.edu.my/7248/, 9 - 11th June, 69 - 72.

Congcong, C., Hou-Min, C., Zhijan, I., Hasan, J. and Zeng, Z. (2013). Sugars Analysis of Hydrolyzate: A Method for Rapid Determination of Sugar in Lignocellulose Prehydrolyzate. *Bioresources,* 8(1): 172 - 181.

Djimtoingar, S. S., Derkyi, N. S. A., Kuranchie, F. A. and Yankyera, J. K. (2022). A review of response surface methodology for biogas process optimization. *Cogent Engineering*, 9(1): 1 – 35.

Dubois, M., Gilles, K., Hamilton, J., Rebers, P. and Smith, F. (1956). Colorimetric Method for Determination of Sugars and Related Substances. *Analytical Chemistry*, 28(3): 350 - 356.

Ebrahimiagda, E. and Ogden, K. I. (2018). Evaluation and modelling of bioethanol yield efficiency from sweet sorghum juice. *BioEnergy Research*, 11: 449-455.

Ezea, I. B. (2023). Technologies and factors affecting bioethanol fermentation and its commercialization. *Archives of Ecotoxicology*, 5(1): 32-36.

Fakruddin, M., Abdu Quayum, M., Ahmed, M. M. and Choudhury, N. (2012). Analysis of key

factors affecting ethanol production by Saccharomyces cerevisiae. *Biotechnology*, 11(4): 248-252.

Farid, T., Dimitar, K. And Irini, A. (2010). Production of Bioethanol from Wheat Straw: An Overview on Pretreatment, Hydrolysis and Fermentation. *Bioresource Technology*, 101: 4744 - 4753.

Ferreira, V., Mariana, O. F., Sabrina, S. M. and Nei, P. (2010). Simultaneous Sacharification and Fermentation Process of Different Cellulosic Substrates using a Recombinant Sachromyces Cerevisiae Harbouring the b-Glucocidae Gene. *Electronic Journal of Biotechnology*, 13: 2.

Fitrriani, K. and Anwar, K. (2013). Hydrolyzate as Raw Material for Bioethanol Production. International *Journal of Advanced Science, Engineering Information and Technology*, 3: 3.

Friedemann, A. J. (2021). Life After Fossil Fuels: A Reality Check on Alternative Energy. *Springer International Publishing*, London, UK.

Garda, M., Ballesteros, I., Gonzalez, A., Oliva, J., Ballesteros, M. and Negro, M. (2006). Effect of Inhibitors Released during Steam-Explosion Pretreatment of Barley Straw on Enzymatic Hydrolysis. *Applied Biochemistry and Biotechnology*, 129(32): 278–288.

Geng, A. (2013). Conversion of oil palm empty fruit bunch to biofuels. Chapter 16, Liquid, Gaseous and Solid Biofuels – Conversion Techniques. *Intech Open* Ltd, London, pp. 480-490.

Helma, K. R. (2013). Review of Research on Production Method of Hydrogen: Future Fuel. *European Journal of Biotechnology and Bioscience*, 1(2): 84 - 93.

Holochek, J. L., Goli, H. M. L., Sawalhah, M. N. and Valdez, R. (2022). A global assessment: Can renewable energy replace fossil fuel by 2050? *Sustainability*, 14:4792., https://doi.org/10.3390/su14084792.

Hu, Z., Wing, J., Kong, H. and Chai, X. (2008). A Novel Method for Determination of Sugars by UV Spectroscopy. *Journal of Chemical Industrial Engineering*, 59(5): 233 - 1237.

Igbokwe, J. O., Onuoha, L. N., Nwafor, M. O. I. and Aviara, N. A. (2019). Characterization of Blends of Petrol and Bioethanol Synthesized from Nigerian Palm Bunch. *Arid Zone Journal of Engineering, Technology and Environment,* 15: 142-152.

Kabue, T. G., Koske, J. and Mutiso, J. (2020). Modeling effects of process variables during fermentation of pineapple peels using the yeast for ethanol production using a second order optimal rotatable design in four dimensions. *Mathematical Theory and Modeling*, 10(6): 1-9.

Kumar, S., Sing, S., Mishra, I. and Adhikari, I. (2009). Recent Advances in Production of Bioethanol from Lignocellulosic Biomass. *Chemical Engineering and Biotechnology*, 32(4): 517 - 526.

Leland, M. V. (2005). A review of pervaporation for product recovery from biomass fermentation processes. *Journal of Chemical Technology and Biotechnology*, 80: 603 – 629.

Liu, R. and Shen, F. (2008). Impacts of Main Factors on Bioethanol Fermentation from Stalk Juice of Sweet Sorgan by Immorbilized

Sacchromyces Cerevisiae (Cicc 1308). *Bioresources Technology*, 99: 847 - 854.

Millati, R., Wikandari, R., Trihandayani, E. Cahyanto, M., Taherzadeh, M. and Nikklason, C. (2011). Ethanol from Oil Palm Empty Fruit Bunch via Dilute Acid Hydrolysis and Fermentation by Mucor Indicus and Saccharomyces Cerevisae, *Agriculture Journal*, 6(2): 54 - 59.

Miller, G. (1959). Use of Dinitrosalycylic Acid Reagent for Determination of Reducing Sugar. *Analytical Chemistry*, 31(3): 426 - 428.

Mingjia, Z., Fang, W., Rongxin, S., Wei, Q. and Zhimin, H. 2010. Ethanol Production from High Dry Matter Corncob using Fed-Batch Simultaneous Saccharfication and Fermentation after Combined Prtreatment. *Bioresource Technology*, 101: 4959 - 4964.

Mishra, A. and Goh, S. (2019). Bioethanol production from various lignocellulosic feedstocks by a novel fractional hydrolysis technique with different inorganic acids and co-culture fermentation. *Fuel*, 236: 544-553.

Mohd, A. K., Loh, S. K., Nasrin, A. B., Astimar, A. A. and Rosnah, M. S. (2011). Bioethanol production from enzymatically saccharified empty fruit bunches hydrolysates using Sacccharomyces cerevisiae. *Research Journal of Environmental Sciences*, 5(6): 573-586.

Nor, A., Mailin, M., Roslindawati, H., Mohd, F., Wan, N. and Kok-Giap, H. (2012). Bio-oils and Diesel Fuel derived from Alkaline treated Empty Fruit Bunch (EFB). *International Journal of Biomass and Renewable Energy*, 1: 6 – 14.

Nurul, A., Nasrin, A., Loh, S. and Choo, Y. (2014). Bioethanol production by fermentation of oil palm empty fruit bunches pretreated with combined chemicals. *Journal of Applied Environmental and Biological Sciences*, 4: 234 - 242.

Petersson, A., Thomsen, M., Hauggaard, H. and Thomsen, A. (2007). Potential Bioethanol and Biogas Production using Lignocellulosic Biomass from Winter Rye, Oilseed Rape and Faba Bean. *Biomass and Bioenergy,* 31: 812–819.

Pradeep, C. M. and Samir, K. K. (2011). Biomass Derived Syngas Fermentation into Biofuels. New York: Academic Press, Elsevier.

Prassad, S., Singh, A. and Joshi, H. (2007). Ethanol as an Alternative Fuel from Agricultural, Industrial and Urban Residues. *Resources Conservation and Recycling*, 50: 1–39.

Richana, N., Winarti, C., Hidayat, T. and Prastowo, B. (2015). Hydrolysis of Empty Fruit Bunches of Palm Oil (Elaeis Guineensis Jacq.) by Chemical, Physical, and Enzymatic Methods for Bioethanol Production. *International Journal of Chemical Engineering and Applications*, 6: 6.

Salakkan, A., Phukoetphim, N., Laopaiboon, P. and Laopaiboon, L. (2023). Mathematical modeling of bioethanol production from sweet sorghum juice under high gravity fermentation: Applicability of Monod-based, Logistic, modified Gompertz and Weibull models. *Electronic*

Journal of Biotechnology, 64: 18-26.

Saud, S., Haseed, A., Anees, S., Zaidi, H., Khan, H. and Li, H. (2024). Moving towards green growth: Harnessing natural resources and economic complexity for sustainable development through the lens of the N-Shaped EKC framework for the European Union. *Resources Policy*, 91: 104804., https://doi.org/10.1016/j.resourpol2024.104804.

Suanes, G., Bolonio, D., Cantero, A. and Yenes, J. I. (2024). Principles for the design of a biomass-fueled internal combustion engine. *Energies*, 17:1700., https://doi.org/10.3390/en17071700.

Tan, K., Lim, S., Low, C. and Chang, S. (2014). Engine emission analysis and performance test with ethanol-gasoline blended fuel. *European International Journal of Science Technology*, 3(7): 9 – 22.

Tran, T. T. A., Le, T. K. P., Mai, T. P. and Nguyen, D. Q. (2019). Bioethanol production from lignocellulosic biomass. Alcohol Fuels: Current Technologies and Future Prospects. Intech Open Ltd, London.

Umikalsom, M., Ariff, B., Zulkifli, H., Tong, C., Hassan, M. and Karim, M. (1997). The Treatment of Oil Palm Empty Fruit Bunch for Subsequent as Substrate for Cellulose Production by Chaetomium Globosum. *Bioresource Technology*, 62: 1-9.

Vasic, K., Knez, Z. and Leitgeb, M. (2021). Bioethanol Production by Enzymatic Hydrolysis from Different Lignocellulosic Sources. *Molecules*, 26: 753. https://doi.org/10.3390/molecules26030753.

Wang, J. And Azam, W. (2024). Natural resource scarcity, fossil fuel energy consumption, and total greenhouse gas emission in top emitting countries. *GeoScience Frontiers*, 15: 101757., https://doi.org/10.1016/j.gsf.2023.101757.

Zhang, J. (2024). Energy access challenge and role of fossil fuels in meeting electricity demand: Promoting renewable energy capacity for sustainable development. *GeoScience Frontiers*, 15:101873., https://doi.org/10.1016/j.gsf.2024.101873.